



Universidad
Carlos III de Madrid



This is the submitted version of the following published document:

Valmorbida, A., et al. Validation of enabling technologies for deorbiting devices based on electrodynamic tethers. In: *Acta Astronautica*, Vol.198, Sept.r 2022, Pp. 707-719

DOI: <https://doi.org/10.1016/j.actaastro.2022.06.013>

© 2022 IAA. Published by Elsevier Ltd. All rights reserved.

Validation of enabling technologies for deorbiting devices based on electrodynamic tethers

A. Valmorbida^{a,b*}, L. Olivieri^b, A. Brunello^b, G. Sarego^b, G. Sánchez-Arriaga^c and E. C. Lorenzini^{a,b}

^a *Università degli Studi di Padova, Dept. of Industrial Engineering (DII), Via Venezia 1, 35131, Padova (Italy),*

^b *Università degli Studi di Padova, Center for Studies and Activities for Space (CISAS), Via Venezia 15, 35131, Padova (Italy)*

^c *Universidad Carlos III de Madrid, Avenida de la Universidad 30, 28911, Leganés (Spain)*

* Corresponding Author, e-mail: andrea.valmorbida@unipd.it

Abstract

The increasing number of man-made objects in near-earth space is becoming a serious problem for future space missions around the Earth. Among the proposed strategies to face this issue, and due to its passive and propellant-less character, electrodynamic tethers appear to be a promising option for spacecraft in low Earth orbits thanks to the limited storage mass and the minimum interface requirements to the host spacecraft.

This work presents the roadmap that the Electrodynamic Tether Technology for Passive Consumable-less Deorbit Kit (E.T.PACK) is following to develop a prototype of a deorbit device based on electrodynamic tether technology with Technology Readiness Level 4 by the end of 2022. The paper illustrates the roadmap of the activities carried out at the University of Padova, where software and hardware have been prepared to validate some of the critical elements of the deorbit device. Specifically, the software tools include: (a) the software called “DEPLOY” that allows the computation of a reference trajectory for the deployment of the tether and the completion of sensitivity analysis of the deployment trajectory to key error sources; (b) the software called “FLEXSIM” that predicts the performances of electrodynamic tethers as a function of the system configuration employed; and (c) the software called “FLEX” that includes the dynamical effects of tether flexibility and provides important information on the dynamic stability of the system during deployment and deorbiting phase. The paper describes in detail the three software tools and provides results of a simulation showing how it is possible to deorbit a 24-kg satellite from an initial orbital altitude of 600 km in less than 100 days using a 500-m long tape-like bare tether.

The team has also developed laboratory mock-ups and performed experimental activities to: (a) determine the tether mechanical properties; (b) test the functionality of mechanisms used to deploy the tether; (c) test the functionality of the attitude control assembly used during the deployment phase; and d) validate a passive damper designed for dissipating the longitudinal oscillations of the tether and thus guarantee the stability of the system during both deployment and deorbiting phase. The paper provides a description of both the laboratory setup and the experimental activities performed to validate EDT technologies, including the damping capability of a compact passive-damping mechanism, showing how it can reduce consistently the peak forces up to about 80%.

Keywords: space tethers, satellite end-of-life disposal, electrodynamic tethers, experimental tests and validation.

Acronyms and symbols

EDT	electrodynamic tethers	LEO	Low-Earth Orbits
E.T.PACK	Electrodynamic Tether Technology for Passive Consumable-less Deorbit Kit	PMD	Post Mission Disposal
E.T.PACK-F	Electrodynamic Tether Technology for Passive Consumable-less Deorbit Kit - Flight	ADR	Active Debris Removal
DKD	Deorbit Kit Demonstrator	FET	Future Emerging Technologies
DK	Deorbit Kit	ILD	Om-Line Damper
EEM	Electron Emitter Module	s/c	spacecraft
DMM	Deployment Mechanism Module	UniPD	University of Padova

l	tether length	e^-	electron
\dot{l}	tether length rate	\mathbf{B}	Earth's magnetic field
θ	tether in-plane libration angle	\mathbf{i}	conventional current
$\dot{\theta}$	tether in-plane libration angle rate	$\hat{\mathbf{r}}$	unit vector from the host s/c to the Earth's center of mass
c	damping coefficients of the tether in-line damper	\mathbf{F}_L	Lorentz force

1. Introduction

The issues related to the presence of man-made objects in near-Earth orbits were firstly addressed by Kessler in the 70s' [1], which stated that without direct action (e.g. by reducing the in-orbit artificial objects net input) the number of in-orbit human-made objects and their fragments could increase exponentially with time, up to quickly exceed the meteoroid background environment. The qualitative description of the cascade "Kessler Syndrome" was later quantified by the author, which confirmed that we are now entering a time when the orbital debris environment will increasingly be determined by random collisions and that we should avoid leaving future payloads and rocket bodies in orbit after the end of their operational life [2]. In fact, the recent constant growth of the small satellite launch rate [3][4] as well as the on-going deployment of several large constellations [5][6] have further distressed the scientific community. In this context, Foreman et al. [7] used the NASA Orbital Debris Engineering Model software and a Monte Carlo analysis to examine the potential implications of two recent satellites constellations by OneWeb and SpaceX on the LEO environment. In addition, Olivieri et al. [8] developed a simple statistical tool for lost vehicles during large constellations life, analyzing the effects of the main parameters of the constellations on its vulnerability.

The sustainability of the access to several Low-Earth Orbits (LEO) is under discussion [9][10][11] and the increasing number of resident objects is enhancing the probability of in-space collisions [12]. It was estimated that in case of future events such as the Cosmos-Iridium collision [13] the generated fragments are not only limited to the altitudes involved but may contaminate neighbouring orbits. In this context the current orbital population is under constant scrutiny, with the development of lists of potential objects whose fragmentation might strongly influence the access to some orbits [14][15][16], the investigation of potential critical fragmentation events [17][18][19], and the definition of strategies for the long-term sustainability of space activities [20].

The scientific community is evaluating mitigation strategies, considering both the utilization of enhanced protections [21] and the implementation of Post Mission Disposal (PMD) [22] and Active Debris Removal (ADR) [23] operations and strategies [24]. In addition, responsible conducts and self-regulations are appearing as promising solutions to address the issue of space debris [25][26]. In parallel, guidelines regarding the deorbiting of all new satellites within 25 years from mission completion, if their deployment orbit altitude is below 2000 km (i.e., in LEO), have been introduced [27] and, in a few cases, they have been absorbed into the countries legal frameworks [28].

The 25 years guideline for spacecraft disposal is currently leading to the development of deorbiting strategies (i.e., by saving propellant for re-entry maneuvers) or to the installation of dedicated systems on board the spacecraft by most of the major providers. Among them, dedicated electrical [29] and chemical [30] propulsion systems were suggested for disposal, as well as drag enhancement devices [31][32] and Electrodynamic Tethers (EDTs) [33][34][35]. In a relevant way, EDTs are a promising option that may overcome the limitations of traditional chemical and electrical propulsion and can potentially be lighter [36] and less prone to debris impact risk [37] [38] than other devices, such as neutral drag sails. In this context, the H2020 project E.T.PACK (Electrodynamic Tether Technology for Passive Consumable-less Deorbit Kit) aims at developing a deorbit kit prototype based on EDT technology [39].

The E.T.PACK consortium is formed by a mix of academia, research centers and companies specialized in the fields required to prove the feasibility of EDT technologies: Universidad Carlo III de Madrid (UC3M)(Spain), University of Padova (UniPD)(Italy), Technische Universitat Dresden (TUD)(Germany), Fraunhofer-Institut für Keramische Technologien und Systeme (IKTS)(Germany), Advanced Thermal Devices (ATD)(Spain) and SENER Aeroespacial (Spain). The consortium has knowledge on Low Work function Tether (LWTs) and plasmas (UC3M), thermionic materials (IKTS), tethers and mechanisms (UniPD), electric propulsion (TUD), solid state devices (ATD) and space product development (SENER). The European Commission invited the E.T.PACK consortium to sign the Grant Agreement of a subsequent EIC Transition project named E.T.PACK-F (Flight), that will increase the TRL from 4 (for the current E.T.PACK) up to 8. A mission demonstrating the kit functionality (DKD – Deorbiting Kit Demonstration) is planned for 2025 [40], just after E.T.PACK-F will be completed, within the framework of a launch agreement signed during IAC 2021 in Dubai between SENER Aeroespacial and Rocket Factory Augsburg.

The University of Padova (UniPD) is one of the partners of the E.T.PACK and E.T.PACK-F projects consortia, both coordinated by the Universidad Carlos III de Madrid. The team at UniPD was tasked with the validation of a certain number of enabling technologies for the deorbit kit including the development of software tools to study the EDT performance and dynamical behaviour and the realization and test of hardware mock-ups and prototypes. In the remainder of this paper, the EDT technology and the E.T.PACK project are presented in Section 2. The roadmap of the University of Padova activities to validate the enabling technologies for the DKD mission is introduced in Section 3. Lastly, the software development and experimental activities are presented in Sections 4 and 5.

2. Electrodynamic tethers and the E.T.PACK project

A modern EDT consists of a long conductive bare tether connecting two spacecraft, usually a host spacecraft and a tip mass. Referring to Figure 1, electrons are passively captured by the bare tether from the ionospheric plasma and

98 are reemitted back into the plasma by using either an active electron emitter (cathode) or a segment of the tether made
99 of a low-work-function material using thermionic emission and photoelectric effects [41][42]. The electric current that
100 flows in the tether interacts with the Earth's magnetic field generating a Lorentz force that, depending on the
101 configuration of the system, can be used to either deorbit the host satellite or to reboost it.

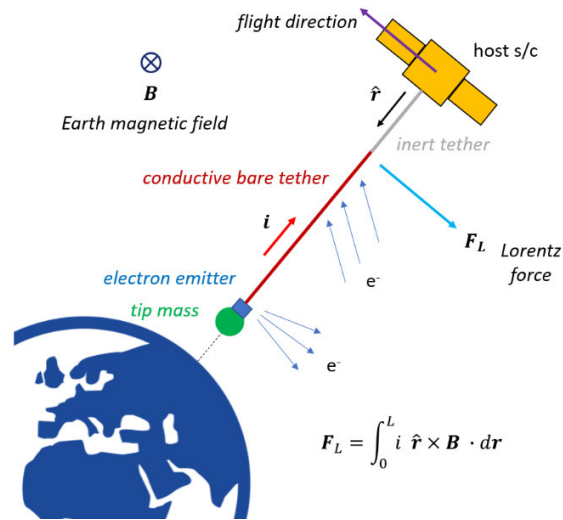
102 The physics of EDTs was first demonstrated in the 1990s with three orbital missions: the two NASA-ASI Tethered
103 Satellite System missions -- TSS-1 (1992) and TSS-1R (1996) -- and the NASA Plasma Motor Generator (PMG)
104 mission (1993). More recently EDT projects have included: NASA's Propulsive Small Expendable Deployer System
105 (ProSEDS) scheduled for 2003 but with the launch cancelled after the Shuttle Columbia accident, and the Naval
106 Research Laboratory (NRL) Tether Electrodynamic Propulsion CubeSat Experiment (TEPCE), launched successfully
107 in 2019 [43].

108 Concerning the tether geometry, round tethers have been employed in several space missions of the past. However,
109 in the last few years it was demonstrated that tape tethers have much better survivability to small debris and
110 micrometeoroids impacts. In this context, Khan and Sanmartin [44] used NASA and ESA debris flux models to develop
111 a simple analytical formulation that can be used as a preliminary design tool [45] for calculating tape tethers
112 survivability per unit length as a function of taper dimensions, i.e., width and thickness, and orbit parameters, i.e.,
113 altitude and inclination. In a recent work [46], Fujiwara et al. used a two-stage light-gas gun to conduct hypervelocity-
114 collision experiments on aluminum tape tethers to assess their survivability against debris collisions. Moreover, tape
115 tethers have better ability for equal tether mass to collect the ionospheric electrons than round tethers, as shown by
116 Sanmartin et al. in [47] and [48]. The ability of a bare tether in collecting electrons from the Earth's ionosphere in LEO
117 was investigated experimentally by Siguier et al. in [49].

118 EDTs are now being developed in Europe, USA, Canada and Japan for the deorbiting of satellites at the end of their
119 operational life with the final aim of mitigating space debris in LEO. Yao and Sands [50] used an EDT system with a
120 500 meter tether charged with a 1 Amp current to increase the orbital altitude by 250 m of a 100 kg spacecraft flying
121 in a LEO orbit (275 km). The University of Michigan [51] is investigating the use of a short (few meters)
122 electrodynamic tether as a technology for propellant-less drag cancellation and orbital change of smartphone-sized
123 spacecraft. They developed the software tool called TeMPEST to predict the propulsion performance of the EDT
124 system for picosatellites (spacecraft mass in the range 100 grams – 1 kg) and femtosatellites (spacecraft mass < 100
125 grams) and are developing the Miniature Tether Electrodynamic Experiment (MiTEE) technology-demonstration
126 mission [52]. In early 2017 the mission called KITE (Kounotori Integrated Tether Experiment) [53] was conducted on
127 the sixth H-II Transfer Vehicle (HTV-6) for demonstrating the maturity of the core technologies for EDTs.
128 Unfortunately, the tether was not deployed due to a mechanical malfunction, but the field emission cathode operated
129 successfully, and the mission demonstrated the maturity of this key technology for EDTs. In addition, this mission
130 confirmed that the deployment of the tether is the first critical phase that requires extensive simulations [54] and
131 laboratory tests [55] to verify the functionality and the reliability of the tip-mass release mechanism and the tether
132 deployment mechanism and control algorithms.

133 Among the other deorbiting technologies, EDTs are an effective and promising technology able to overcome the
134 limitations of traditional active technologies for deorbiting, i.e., chemical or electrical propulsion systems. Tether
135 systems are mostly passive and in the configuration under development (e.g., E.T.PACK) they are designed to be
136 autonomous and independent of the host satellite. In addition, an EDT can control the electric current by inserting a
137 resistor with variable electric resistance between the bare tether and the electron emitter (cathode device) [56].
138 Moreover, if the activation of the current through the conductive tether is properly phased by electrically connecting
139 or disconnecting the cathode device from the tether, the deorbiting profile can be controlled to avoid the collision with
140 catalogued objects (with a characteristic size > 10 cm) [37][57]. The limitation of the current flowing in the tether is
141 also required to limit excessive tether libration during the deorbiting phase that could lead to dynamics instability of
142 the system (flip upside down) before its reenter in atmosphere. In addition, the probability of a tether cut due to very
143 small debris is not a critical issue when using thin tapes as opposed to cylindrical tethers [58].

144 Due to those considerations, EDTs offer a solution that, specifically for LEO satellites and spent stages, is
145 potentially very competitive among the alternative technologies currently used for end-of-life deorbiting missions,
146 hence providing a propellant-free and fully-green device that offers a safe preservation of the space environment.



148
149

Figure 1: working principle of EDT in the configuration with an active electron emitter. The configuration shown in the figure refers to a prograde orbit (inclination < 90 deg) and i indicates the conventional current*.

150
151
152
153 The European Commission funded in 2018 with 3 M€ the project E.T.PACK, that is a 45-month H2020 Future
154 Emerging Technologies FET-OPEN project with the objective of developing an electrodynamic-tether-based Deorbit
155 Kit (DK) with TRL equal to 4. The E.T.PACK consortium has recently finished the design of a Deorbit Kit
156 Demonstrator (DKD) prototype and is carrying out the manufacturing and testing phases of its elements [59]. The
157 DKD consists of a 12U CubeSat with a total mass of 24 kg, that incorporates the key technologies to be validated in
158 space. The flight model of the DKD (to be developed with the E.T.PACK-F project) will be launched into a circular
159 orbit at an altitude of 600 km and a medium inclination, and it will deploy a 500-m-long tape tether. The natural
160 deorbit time of the system from this orbit is more than 15 years (depending on solar activity) and the expected reentry
161 time into the atmosphere using the EDT technology is less than 100 days.

162 The DKD consists of 2 modules connected together [59]: the Deployment Mechanism Module (DMM), that hosts
163 the 500-m tape tether and the Deployment Mechanism (DM), and the Electron Emitter Module (EEM), that hosts the
164 Electron Emitter, an active device that provide the emission of electrons in the plasma environment in order for the
165 current to be established through the tether. Each module is completely independent with their own power,
166 communication, data handling and attitude control subsystems. The mission operations include two phases: a
167 deployment phase, during which the two modules are separated in less than an orbit to reach the nominal configuration
168 with the tether close to the local vertical (see Fig. 1), and the deorbiting phase during which the electrodynamic
169 functionality is enabled for deorbiting.

170
171 **3. University of Padova roadmap to validate EDT technologies**
172 The contributions of the University of Padova (UniPD) to the E.T.PACK project are several and include both
173 software development for EDT applications, hardware development and laboratory testing. Figure 2 shows the
174 roadmap of the UniPD activities to validate the technologies on which the DKD prototype is based. In the next sections,
175 the main steps of the roadmap are described in detail.

176

* related to the movement of positive charges, as it was believed in the 19th century.

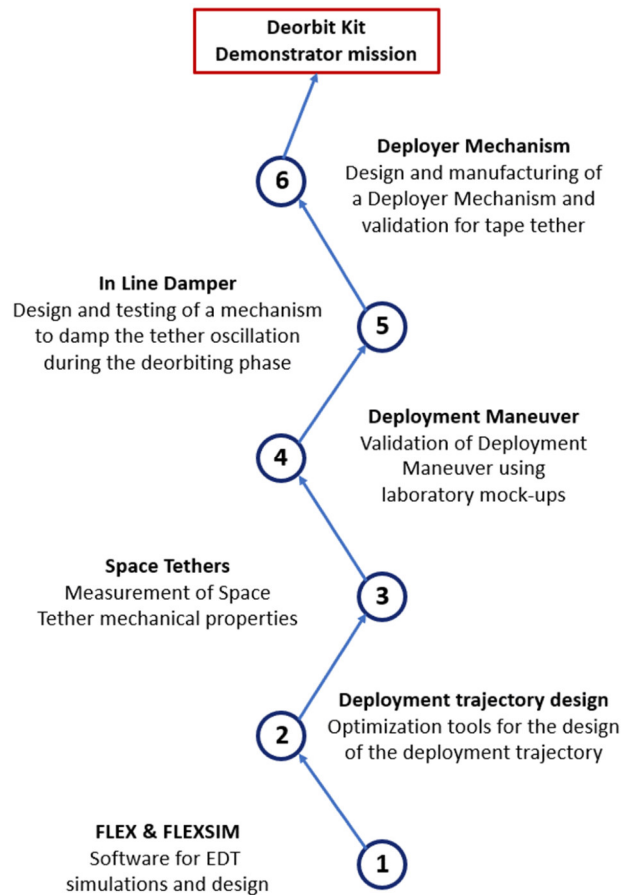


Figure 2: roadmap of the University of Padova’s activities for EDTs.

177
178
179 **4. Software tools for EDT**

180 *4.1 Deployment trajectory design tools*

181 The deployment dynamics of a tethered system is highly nonlinear [60][61][62] and the Coriolis accelerations
 182 acting on the tip masses leads to a configuration of the tethered system with libration amplitudes that are typically in
 183 the range 40°-50° if uncontrolled [63]. Consequently, the first step in the design of a deployment trajectory is to
 184 compute tether length and velocity time profiles that bring the system from given initial conditions to a small libration
 185 amplitude at the end of the deployment maneuver. The equations of motion of a variable-length tether orbiting system
 186 are nonlinear with varying time coefficients. For this reason, we develop a software package based on optimization
 187 tools to solve a boundary value problem of the nonlinear dynamic system to find the trajectory in the system state
 188 space, i.e. tether length l , length rate \dot{l} , libration angle θ and libration rate $\dot{\theta}$, that the tether must track to attain the final
 189 desired state.

190 The reference profiles for the deployment maneuver were first obtained using the BOCOP[®] software [64], and then
 191 fine-tuned in the code *DEPLOY*, developed in MATLAB[®], to smooth out the tether tension profile mainly at the end
 192 of deployment [65]. The equations of the deployment dynamics implemented in the software tool *DEPLOY* can be
 193 found in [65]. The three main steps followed to obtain the deployment reference profiles are shown in Figure 3, where
 194 the block “Nonlinear boundary value problem” implements the differential equations describing the deployment
 195 dynamics for tethers and uses the BOCOP[®] software to find a reference trajectory for deployment that satisfies the
 196 following boundary conditions: initial conditions on l , \dot{l} , θ and $\dot{\theta}$, final conditions on l and \dot{l} , minimizing the final
 197 libration angle and libration rate θ_f and $\dot{\theta}_f$, respectively. Additional details can be found in [65].

198 During the design of the deployment trajectory both tether flexibility end effects of the environmental perturbations
 199 are neglected. Despite this, the simplified mathematical model used to compute the reference deployment trajectory
 200 can catch the key effects that actually drive the deployment dynamics and, as discussed and shown in [65], both tether
 201 flexibility end effects of the environmental perturbations can be neglected. Indeed, the tether is maintained taut during
 202 the deployment, so the tether bending and its effects on the deployment dynamics is rather limited. In addition, the

203 environmental forces during deployment are negligible, since: (a) the Lorentz force is null during deployment because
 204 the electron emitter (cathode) is not enabled until the following deployment phase; (b) the aerodynamic drag is
 205 negligible at an orbital altitude of 600 km; and (c) the effects of solar radiation pressure are negligible over the short
 206 deployment time, which is about 1 hour for the E.T.PACK DKD mission.

207 Figure 4 shows an example of reference profiles for the tether length and length rate as a function of time. Figure
 208 5 shows an example of reference trajectory for the deployment of the DKD in the orbital plane. In addition, the UniPD
 209 team developed a MATLAB[®] tool to carry out a sensitivity analysis of the reference trajectory to key error sources:
 210 (a) errors in the release angle between the two modules at the start of deployment, and (b) errors in the deployer
 211 mechanism ability to follow a reference length rate profile for the deployment of the tape tether.

212 Preliminary experimental tests on the deployer control motor showed that it can track the reference length rate
 213 profile for the deployment of the tape with an error that can be modelled as the sum of two components: a bias
 214 component of 0.3 mm/s, which could be due to a dc offset, and a random component with a standard deviation of 1.4
 215 mm/s, which is due to the resolution of the encoder installed on the motor and the feedback control law of the motor.
 216 This leads to a final error on the tape deployed length of 1.2 m, i.e., an error of 0.24% over 500 m of total length
 217 (Figure 6). A sensitivity analysis of both the error in the initial release angle and the errors of the deployer mechanism
 218 control showed that the reference trajectory is stable and that the post-deployment in-plane libration amplitude remains
 219 confined within 3 deg (Figure 7) off the local vertical.
 220

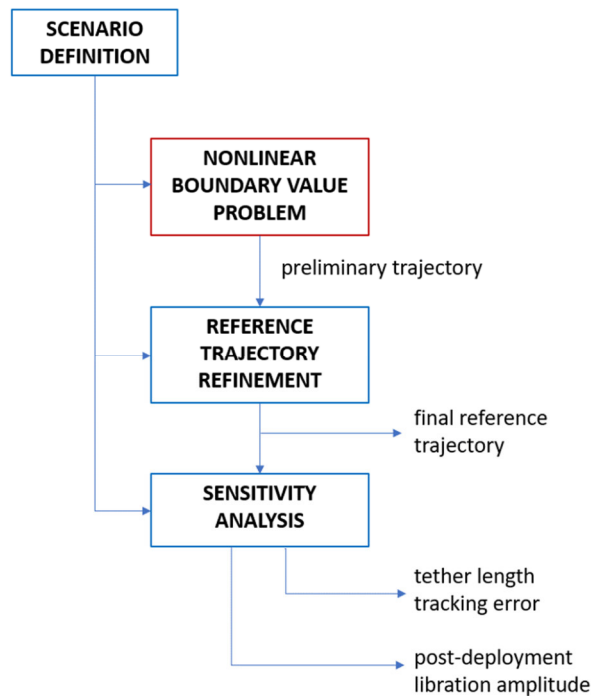


Figure 3: main steps for the design of the deployment reference trajectory.

221
 222
 223
 224

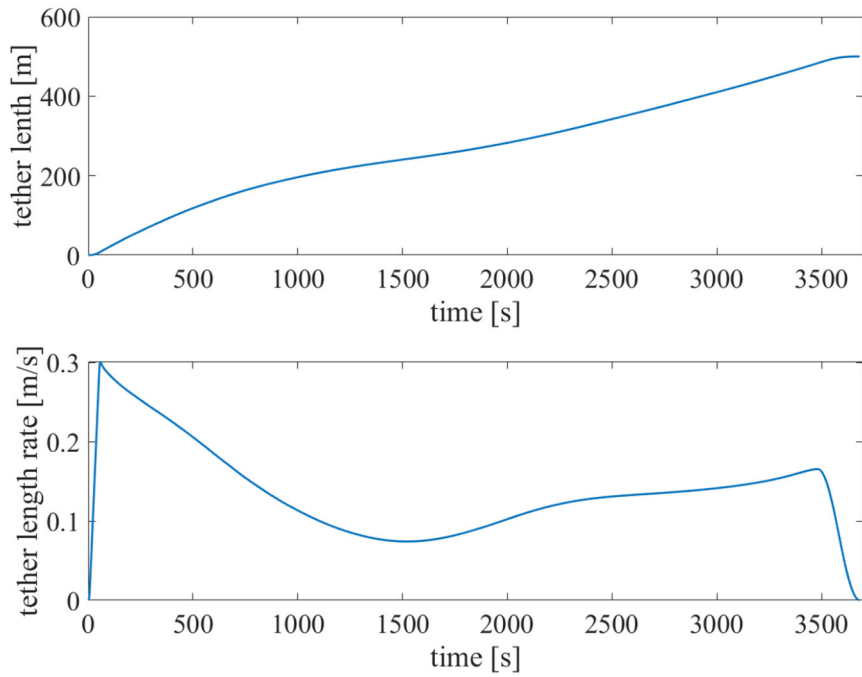


Figure 4: tether length (top panel) and length rate (bottom panel) reference profile.

225
226
227

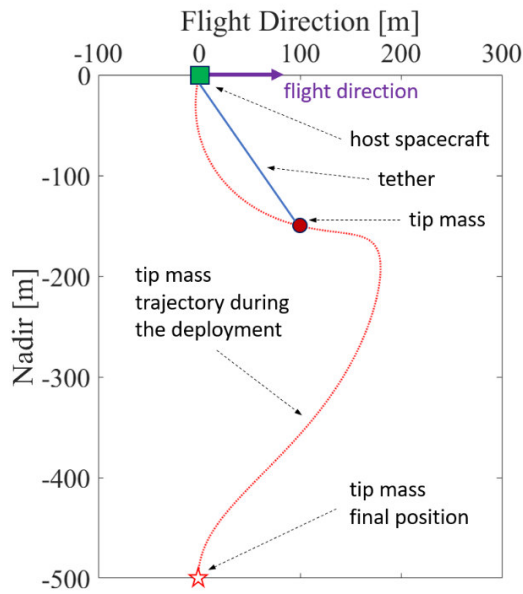


Figure 5: reference deployment trajectory in the orbital plane for the DKD demonstration mission as seen from the host spacecraft. The tip mass is the EEM of the DKD and the DMM is attached to the host spacecraft.

228
229
230
231

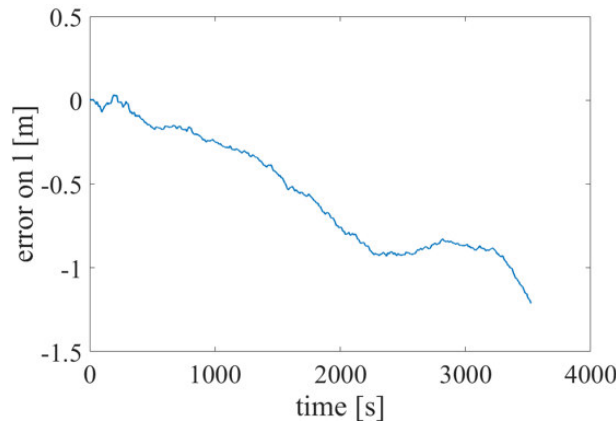


Figure 6: time profile of the deployment length error.

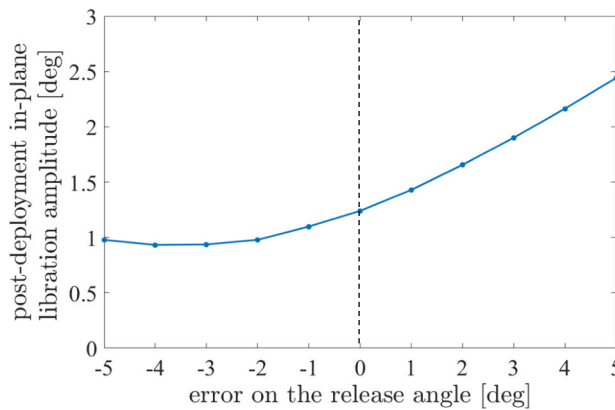


Figure 7: post-deployment in-plane libration amplitude vs. error in the release angle at the beginning of the deployment maneuver. This figure includes the effects due to errors of the deployer mechanism motor in following the reference length rate profile.

4.2 FLEXSIM and FLEX software

Two numerical software packages have been developed through the years for simulating the deorbiting performance of tethered satellite systems at Padova University: *FLEX* and *FLEXSIM*. The former has been under development since the BETs project [66], that was granted under the “FP7-SPACE program in the years 2010-2014. The latter has been developed entirely within the E.T.PACK project with the goal of obtaining faster results of the deorbiting performance of a system without taking into consideration the tether librational and flexible dynamics. Specifically, the fidelity of the simulation results is provided by *FLEX*, which considers both tether libration and flexibility. Since *FLEXSIM* has a much shorter computational time when compared to *FLEX*, *FLEXSIM* is used as a preliminary fast design tool for EDT systems, allowing to compare different system configurations, as for instance different tether lengths, in terms of deorbiting time. Once a good EDT system configuration for a given target satellite is identified, *FLEX* is employed to validate that configuration also considering the effects of tether flexibility and libration.

4.2.1 FLEX

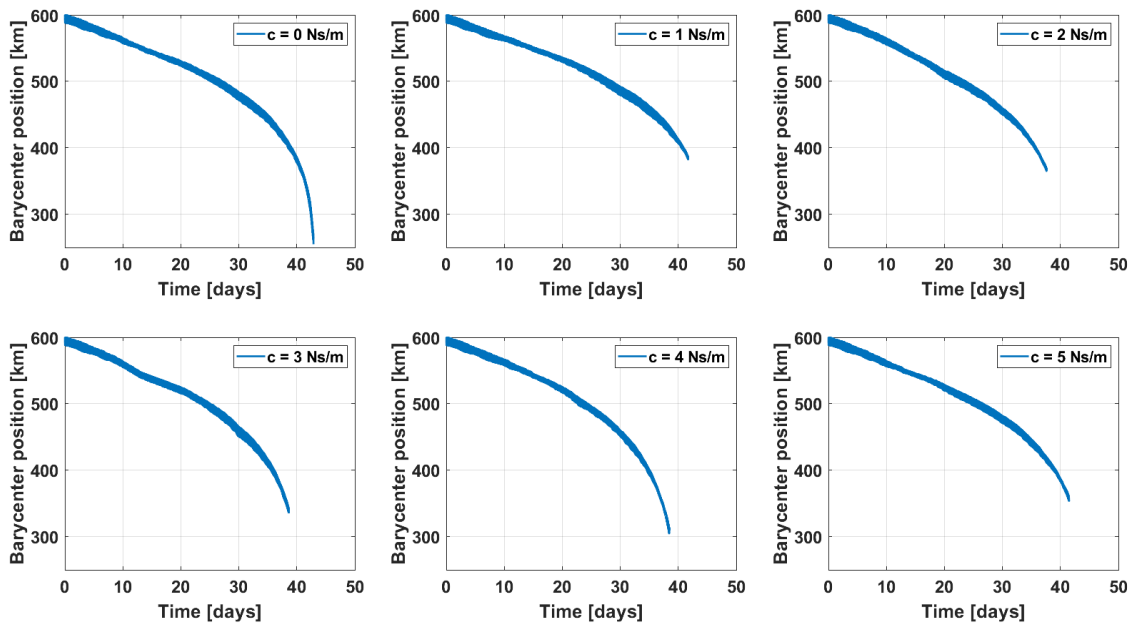
FLEX is a FORTRAN simulator able to describe the dynamics and thermal behaviour of a tethered space system, including the dynamical effects of tether flexibility that are important during deorbiting. On the other hand, once the system is properly designed to provide stability and the aim of the study is the evaluation of the overall deorbiting time, the flexibility can be neglected in favour of a faster computation time.

Thanks to the incorporation of flexibility in the tether model, *FLEX* is able to provide important pieces of information on the dynamic stability of the system during the deorbiting phase. Consequently, *FLEX* is among a few simulators in the world that is able to drive the tether design (e.g., tether mass and electrical properties, tether geometry, tether optical properties and temperature) and able to confirm the long-term stability of the system configuration. An example of this type of study is shown in Figure 8 where different deorbiting times for tethered systems were evaluated after varying the damping coefficients of the in-line damper [67][68]. For all the simulations the limit height at which

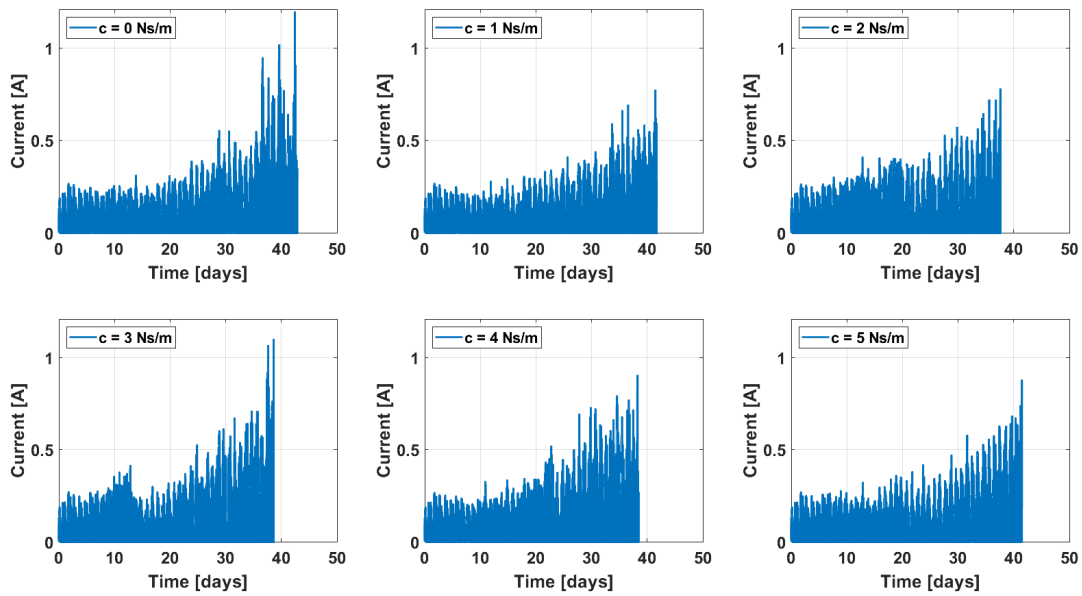
263 deorbiting is ideally considered concluded is 250 km. However, some simulations don't reach this low altitude because
 264 the systems flip upside down at very low altitudes due to the atmospheric drag that creates a torque around the center
 265 of mass of the EDT system. Nevertheless, it is evident that, flipped or not, the systems can be treated as successfully
 266 deorbited in all cases, because below 400 km the atmospheric drag on the tethered system will complete deorbiting in
 267 a few days. Specifically, looking at the top left panel of Figure 8, it is evident that the deorbiting altitude curve is
 268 characterized by two main parts with different slopes. At the beginning of the deorbiting phase, from 600 km to about
 269 400 km, the deorbiting rate is driven by the Lorenz force; on the contrary, when the barycenter position of the system
 270 is below 400 km, the curve experiences an evident change in slop, because the deorbiting rate is now driven by the
 271 atmospheric drag and the tethered system reenters in a few days.

272 Another example of the capabilities of *FLEX* is shown in Figure 10, where the changing tension profile of the tether
 273 at the passage from the illuminated side to the eclipse condition is captured and it shows that the transition needs to be
 274 treated accurately, even though it takes less than 30 seconds.

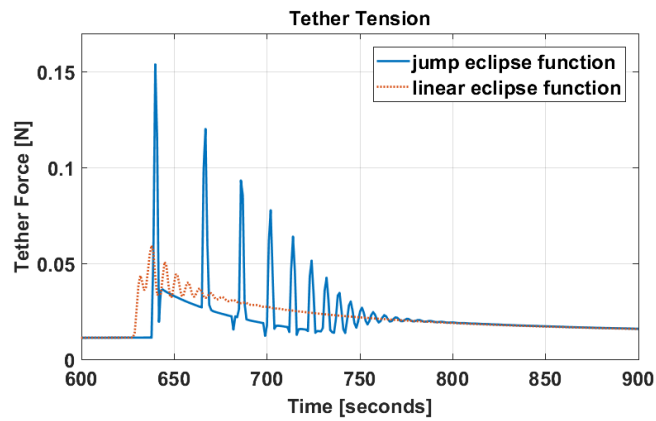
275 As it can be seen from Figure 11, the tether in *FLEX* is discretized into lumped masses connected by a series of
 276 massless springs and dampers [69] that represent the tether mechanical characteristics. Specifically, the dynamics of
 277 this discretized lumped masses model is governed by a set of ordinary differential equations that considers the resulting
 278 force F_i acting on each mass and with constraint conditions related to the continuity of the tether [70]. The resulting
 279 force F_i is the sum of the following contributions: gravitational force, aerodynamics force, Lorentz force, forces due
 280 to thermal elongation or restriction of the tether and elastic forces due to the interaction of each lumped mass with the
 281 neighboring lumped masses. In addition, *FLEX* computes the temperature of the tether by also implementing a thermal
 282 model that considers infrared end visible thermal fluxes due to Earth and Sun. As for the tether current evaluation, the
 283 high-bias Orbital Motion Limited law is used to evaluate the current collection by the bare segment [56].
 284



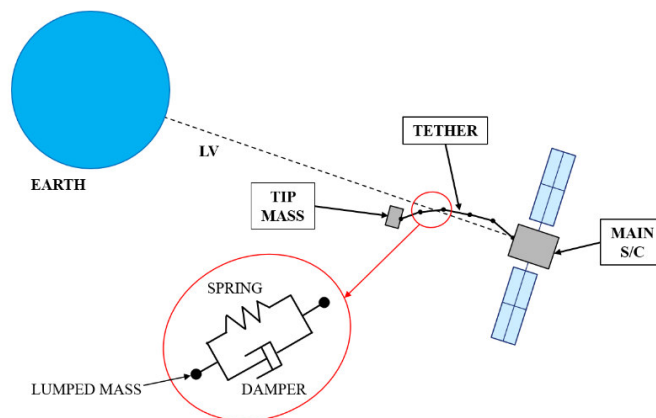
285
 286 Figure 8: deorbiting time for electrodynamic tethered systems with different damping coefficients c of the tether in-
 287 line damper.
 288



289
 290 Figure 9: time profile of the mean electric current through the tape tether during the deorbiting for the six
 291 configurations of the tethered system with different damping coefficient c .
 292



293
 294 Figure 10: tension peaks due to the lit to eclipse transition. The difference is due to the different type of transitions,
 295 over a time less than 30 s.
 296



297
 298 Figure 11: discretized lumped-mass model for the tether in *FLEX*.

299 The following environmental models, originally implemented in Fortran, are incorporated in the code:
 300 1. International Reference Ionosphere IRI-95 [71];
 301 2. International Geomagnetic Reference Field – IGRF [72];
 302 3. NRLMSISE-00 Atmospheric Model [73].

303 As for the thermal model, thermal fluxes coming from the Earth and Sun are taken into consideration together with
 304 the IR emitted radiation for the computation of the tether temperature. *FLEX* has been built with an approach aiming
 305 at flexibility and modularity in order to evaluate satellite performance in a variety of scenarios. With this idea in mind,
 306 gravitational and magnetic field models with different complexity have been implemented and can be activated or
 307 deactivated based on the aim of the individual simulations. Specifically, gravitational models in *FLEX* can be simply
 308 a spherical model or a combination of this J_0 -model with: (1) higher Earth’s gravity harmonics up to the 4th order, (2)
 309 third body gravity perturbations due to Sun, and (3) Moon. Similarly, the magnetic field model can be chosen among:
 310 (1) dipole magnetic field, (2) tilted dipole magnetic field, and (3) a full IGRF model.

311 Lastly, there is a feature in *FLEX* that triggers the limitation of the current flowing in the tether to limit excessive
 312 tether dynamics during the deorbiting phase.

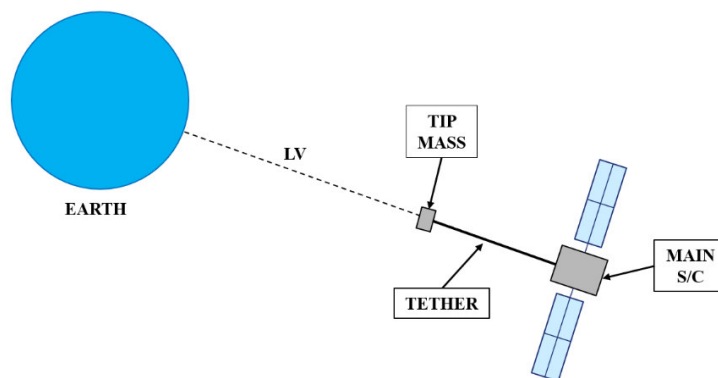
313 The numerical integrator of this simulator is “RADAU5” [74], that employs an implicit Runge-Kutta method
 314 (Radau IIa) of order 5 (three stages) with step size control and continuous output. This code is typically employed for
 315 solving differential equations, such as those describing the flexible tether satellite system that involves phenomena at
 316 different time scales (i.e., orbital motion, tether librations, bending modes, and longitudinal oscillations).
 317

318 **4.2.2 FLEXSIM**

319 *FLEXSIM* is a simulator able to describe the dynamics of a tethered space system, in which the dynamical effects
 320 of tether flexibility and librations are neglected. Figure 12 shows the configuration implemented in *FLEXSIM*: the
 321 tether is considered as a single unit, with equivalent properties computed as if the tether were perfectly aligned with
 322 the local vertical (LV). No in-plane or out-of-plane dynamics is allowed. This model does not distinguish between
 323 conductive and non-conductive portions of the tether, even though equivalent parameters are used consistently.

324 This code is therefore able to evaluate the deorbiting performance of the system in a much shorter computational
 325 time when compared to *FLEX* with the basic assumption that the tether was properly designed to provide stability.
 326 Depending on the orbit inclination, the results might slightly underestimate the deorbiting performance of the system
 327 evaluated by *FLEX* because the out-of-plane dynamics contributes to an increase of the motional electromotive force
 328 that drives on average a higher current flowing in the tether.

329 *FLEXSIM* has the additional feature to let the user choose between a stiff solver (“RADAU5”, the same as *FLEX*)
 330 or a non-stiff solver (“DOPRI5” [75]). Further details can be found in [70].
 331
 332

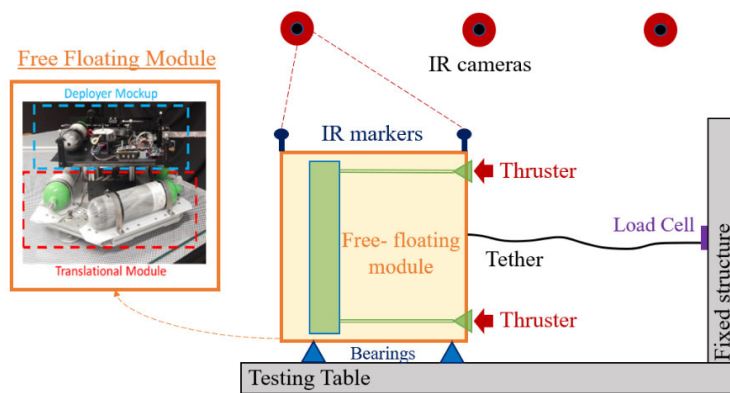


333 Figure 12: tethered satellite model in *FLEXSIM*: the tether dynamics is not modelled; the tether is always unstretched
 334 and aligned with the local vertical.
 335
 336
 337
 338
 339
 340
 341

342 **5. Experimental activities**

343 To validate the main technologies involved in the E.T.PACK project, a series of experiments was performed at the
 344 University of Padova. The test activity was performed in the SPARTANS facility laboratory [76] [77], consisting of a
 345 2-m x 3-m zero-friction testing table with a free floating module (Figure 13). The Module is composed of a translational
 346 module and a mock-up of a tether deployer and its motion is tracked by a set of IR cameras aimed at spherical IR
 347 markers placed on the module. The whole free-floating system has a mass of about 25 kg and three Degrees of Freedom
 348 (DoF), of which two translational DoF are related to its motion on the testing table and one rotational DoF associated
 349 with its rotation around the vertical axis. For the testing activities, the deployer mechanism release a tape/tether whose
 350 length is controlled by the onboard computer to follow a precomputed deployment profile. In addition, the other end
 351 of the tether is connected to a load cell constrained to the testing table structure and utilized to directly measure the
 352 tether tension during deployment.

353 The following subsections focuses on: (1) the determination of the mechanical properties of the tapes employed in
 354 the E.T.PACK projects, (2) the testing and validation of both deployment mechanism and maneuvers for the tether
 355 deployment mock-up, and (3) the development of an in-line damper to damp out tethers oscillations.
 356



357 Figure 13: layout of the experimental setup with the free-floating module, the tether line, and the load cell.
 358
 359

360 *5.1 Tape mechanical properties determination*

361 The aim of this activity was the comparison of different tether materials to find valid solutions for future space
 362 tethered missions. Mission requirements, such as the survivability to hypervelocity impacts and the ability of a tether
 363 material to damp oscillations that arise during both tether deployment and deorbiting maneuvers due, in the latter case,
 364 to the continuous input of energy from the Lorentz forces, affect the tether material and its geometry. Round tethers
 365 have been employed in several space missions of the past. However, in the last few years it was demonstrated that tape
 366 tethers have much better survivability to small debris and micrometeoroids impacts.

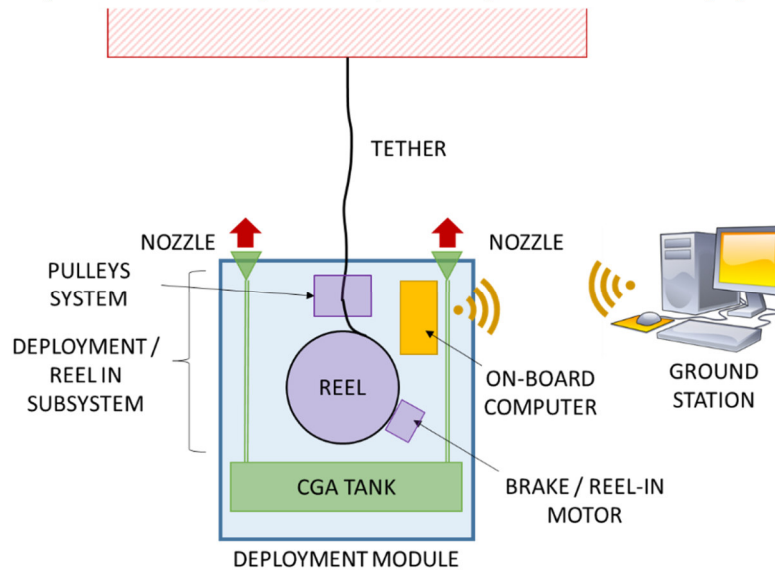
367 In this work, four different tethers were investigated: a round-wire Nylon line, a Spectra braided thread, and two
 368 tape tethers respectively made of PEEK and Aluminium. The determination of their mechanical properties was carried
 369 out through a series of experiments. Specifically, tether stiffness and damping coefficients were evaluated by applying
 370 different tensile load profiles to the free-floating module of the SPARTANS facility and then measuring the tether-line
 371 dynamic response in terms of tension spike amplitude, oscillation decay, and estimation of the damping coefficient. In
 372 the experimental setup, the tether was connected to the free-floating module and to the fixed load cell, that measures
 373 the tether tension during experiment, placed between the tether and a fixed structure mounted on the testing table.
 374 Table 1 summarizes the results obtained, in term of stiffness and damping coefficient, for the four materials
 375 investigated. Further information on tapes stiffness and damping coefficients can be found in [78].

376 Table 1. Space tether mechanical properties determined experimentally.

Materials	Stiffness	Damping coefficient
Nylon	167.6 N/m	8.2 Ns/m
Spectra™	753.4 N/m	35.1 Ns/m
Al-1100	24734.3 N/m	48.2 Ns/m
PEEK	1810.9 N/m	0.37 Ns/m

377 5.2 Validation of early deployment maneuvers

378 Following the heritage and the experience collected in past projects on tether deployment systems [79][80], a
 379 deployer mock-up was designed for the SPARTANS facility to validate in the laboratory scaled deployment maneuvers
 380 based on the E.T.PACK reference profiles [65]. We must point out that the deployer mechanism that was tested
 381 employed a rotating reel from which the tape tether is extracted using a drive-pulleys system. Although this deployment
 382 mechanism is not the one finally chosen in the DKD of E.T.PACK, the drive-pulleys system is representative of the
 383 tether deployment dynamics, because the dynamics of the tether outward of the drive-pulleys system is decoupled from
 384 the internal dynamics of the rotating reel. A first configuration of the deployer mechanism is sketched in Figure 14. It
 385 consists of a Cold Gas Actuator (CGA) propulsive unit, employing two nozzles, a pressurized tank, the associated
 386 fluidic system, and a deployment and reel-in subsystem, composed by a rotating reel, a system of drive pulleys to
 387 control the tape deployment, and a motor coupled to the reel to keep the inner part of tether taught during deployment
 388 and retrieve it during reel-in operations. In the laboratory configuration, the whole module can act as tip mass during
 389 deployment, as well as to perform the reel-in operations by switching the motor function [81].



390 Figure 14: sketch of the lab deployment module [81].
 391
 392
 393

394 The following activities were performed with the mock-up in the SPARTANS facility. First, a controlled
 395 deployment test demonstrated the system capability to reel-out the tape following a reference trajectory during the
 396 early separation phase. As expected, the angular acceleration of the tape coil affected the attitude of the deployment
 397 module but did not influence the deployment profile. Similarly, a reel-in test (Figure 15) demonstrated the capability
 398 of the proposed system to retrieve the tape [81].

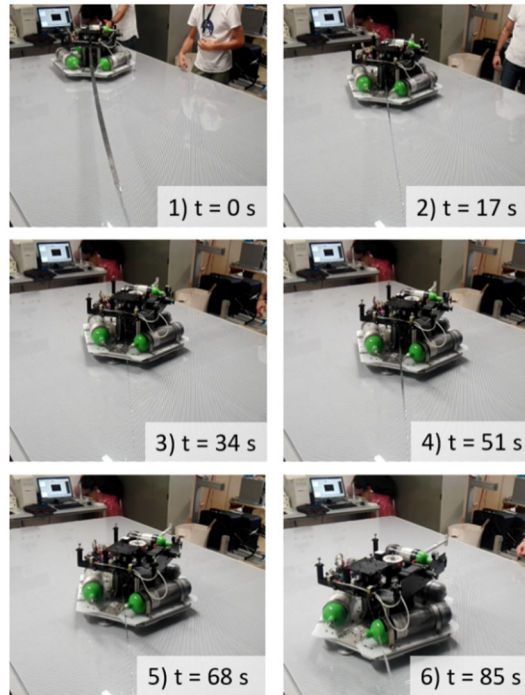
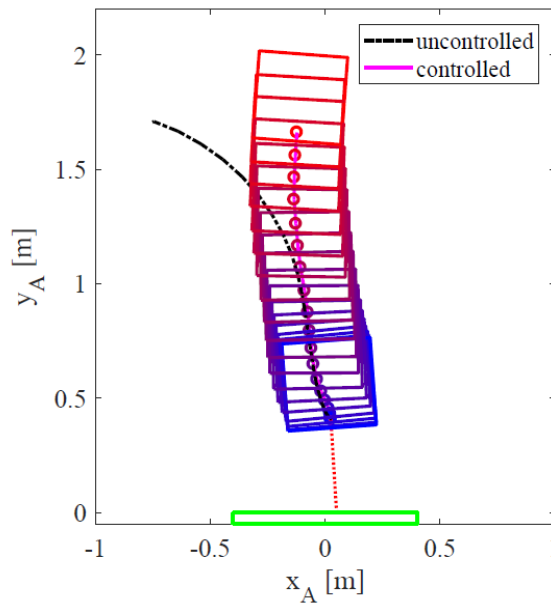


Figure 15: pictures from the tested reel-in procedure [81].

399
400
401
402
403
404
405
406
407
408
409
410

To overcome the issue of attitude deviations, dedicated attitude thrusters were actuated for controlling the module. The deployment procedures were replicated while keeping the module aligned with the tether deployment direction within a dead band of ± 10 deg [82]. Figure 16 compares the reconstructed deployment procedures for the original uncontrolled scenario and the system with the attitude control operating. It can be noted that the system is capable of maintaining the alignment and performs the maneuver; further details on the system can be found in [82]. Lastly, the facility was employed to test a prototype of a passive in-line damper developed by the University of Padova for reducing the oscillations of the tape tether during the deployment maneuver [65]. Tests showed that the prototype can smooth out impulsive loads and damp transient events, allowing for smoother operations by dissipating oscillations.

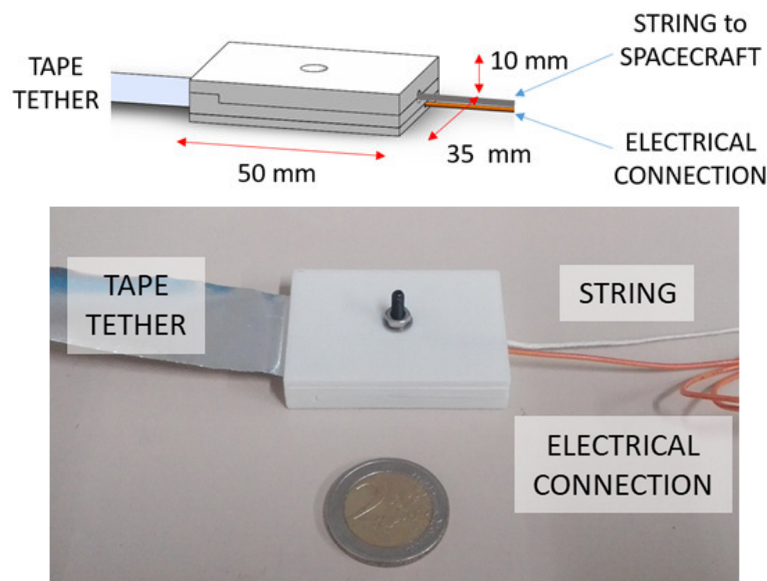


411
412

Figure 16: comparison of deployment procedures without and with the attitude control [82].

413 5.3 Development of an in-line damper

414 The dynamical stability of a tethered system can be strongly affected by the deployment strategies [83] and
 415 environmental disturbances during deorbit [84][85][86]. Consequently, it is necessary to implement energy dissipation
 416 strategies to reduce the amplitude of the tether oscillations to guarantee the stability of the system during both
 417 deployment and deorbiting phases. Among the possible solutions for passive dissipation, elastic damping materials are
 418 incorporated in series to the metallic tape; the E.T.PACK DKD is expected to include a section of 100 m of PEEK to
 419 reduce libration and oscillations. To further dampen the tether dynamics, it is planned to include an in-line damper
 420 (ILD), consisting in a small mechanism utilizing viscous-elastic devices. For the DKD, the University of Padova is
 421 proposing a compact ILD suited for CubeSat-sized tethered systems, to be placed between the tip mass and the tether
 422 and designed to absorb and smooth out tensile loads transmitted by the tether [67]. The ILD is designed to fit on board
 423 the DKD. The device has a volume of $50 \times 35 \times 10 \text{ mm}^3$; in addition to its damping capability, it provides an electrical
 424 connection between the tether and the module at the tip. A drawing and a picture of the ILD can be seen in Figure 17.
 425 A patent application was submitted in 2021 for this device.
 426



427
 428 Figure 17: external case of the ILD with the main connection elements
 429
 430

431 The ILD was subjected to a number of tests [67] with the SPARTANS facility to verify its mechanical
 432 characteristics in terms of stiffness and damping coefficient. During the test campaign, the ILD was fixed to the
 433 SPARTANS module (see Figure 13) and a string of known length connected the ILD to the load cell constrained to
 434 the fixed structure. In all experiments the string was slack at the start of experiment, to allow an initial acceleration of
 435 the free-floating module pushed by the cold gas unit. A first test investigated the response to a single impulse by
 436 switching the thrusters on for a short time (about 1 second) and switching them off before the string could be stretched.
 437 A second set of experiments was performed to assess the response of the system to a step load given by leaving the
 438 thrusters switched on; a third test investigated the response to pulsed loads given by continuously switching on and off
 439 the thrusters. All cases were compared to experiments without the ILD, indicating a consistent reduction in peak forces:
 440 from about 80% for single impulse tests to about 30% for pulsed loads experiments. A selection of the tests results in
 441 terms of load measured by the load cell can be seen in Figure 18. From the analysis of the experiments data, the
 442 resulting values of the ILD stiffness and damping coefficient were respectively 160 N/m and 43.0 Nm/s.
 443

444 Last, the tether deployment manoeuvre tested in section 5.2 was replicated placing the ILD close to the fixed load
 445 cell. Results [67] showed a consistent reduction in transient loads peaks, confirming the capability of the ILD to
 dampen transient loads.

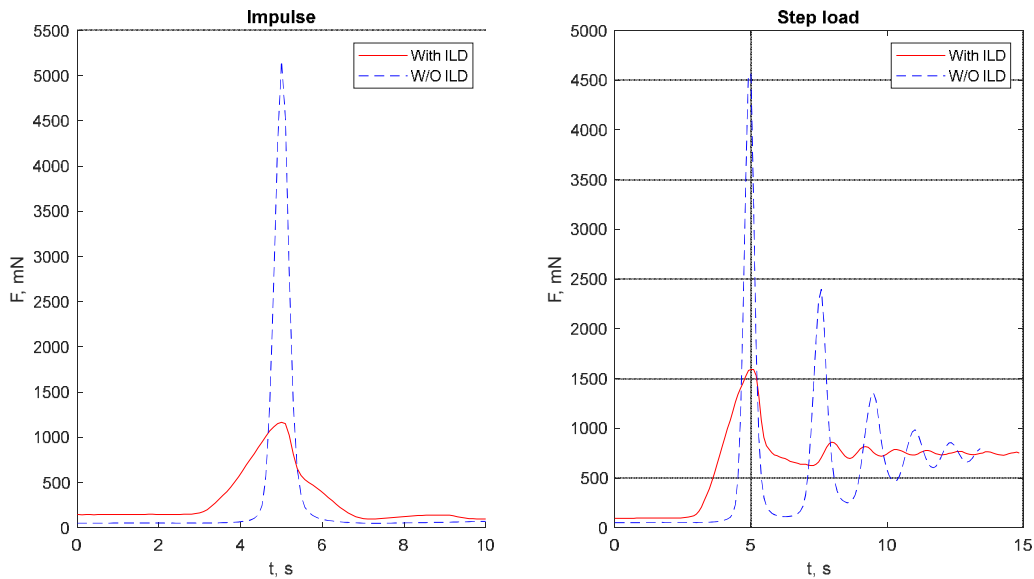


Figure 18: load cell measurement: comparison of tests without (dashed blue line) and with ILD (solid red line) for the response to a single impulse (left) and to a step load (right).

6. Conclusions

This article explains the roadmap of the activities conducted at the University of Padova to validate the technologies on which the Deorbit Kit Demonstrator (DKD) prototype of the E.T.PACK project is based. The contributions include software development for Electrodynamic Tether (EDT) applications, hardware development and laboratory testing that validate experimentally the technologies required in the phases of deployment and deorbiting of an EDT system.

Concerning software development, two kind of software tools were developed. The first one, DEPLOY, is utilized to compute the reference trajectories for the deployment phase of the DKD mission, and also to run a sensitivity analysis to errors on both the initial release angle and the capability of the deployer mechanism to track the reference profile. The second set of software tools includes FLEX and FLEXSIM simulators that contributed to defining the proper design of an EDT system, compute the deorbiting performance, and provide essential information on the dynamic stability of the system during the deorbiting phase. Specifically, FLEX is a high-fidelity simulator for EDT systems that implements: a) the orbital dynamics of the tether, b) the libration dynamics and the flexibility of the tether, c) the thermal fluxes on the tether due to infrared and visible radiations in orbit, allowing the computation of the tether temperature, d) the exchange of electrons between the tether and the ionosphere, permitting the evaluation of the electric current through the tether during the deorbiting phase, and e) the interaction with the Earth magnetic field for the generation of the Lorentz force.

Concerning the experimental activities performed to validate EDT technologies, the E.T.PACK team of the University of Padova carried out laboratory tests in order to first estimate the mechanical properties of the tapes employed in the E.T.PACK prototype in terms of elastic modulus and damping coefficients. A reliable estimation of the mechanical properties of the tether materials are very important, because they contribute to influence the stability of the tether during the deployment and the deorbiting phases. In addition, a laboratory mock-up was developed and employed to validate the design of a drive-pulleys system used during the early and critical phase of deployment. This technology was tested using a free-floating module and the low-friction facility called SPARTANS of the same institution that reproduces the microgravity environment typical of satellites in orbit. Moreover, the same team developed a compact passive-damping mechanism used to increase the stability of the tethered system during both deployment and deorbiting phases. The damping capability of this compact mechanism was tested using the low-friction facility and the experimental tests showed that the in-line dumper can smooth out impulsive loads and damp transient events, reducing consistently the peak forces, from about 80% for single impulse tests to about 30% for pulsed loads experiments.

Acknowledgements

This work was supported by European Union's Horizon 2020 Research and Innovation Programme under Grant Agreement No. 828902 (3M€ E.T.PACK Project).

483 **References**

- 484
- 485 [1] Kessler, D. J., & Cour-Palais, B. G. (1978). Collision frequency of artificial satellites: The creation of a debris
486 belt. *Journal of Geophysical Research: Space Physics*, 83(A6), 2637-2646.
- 487 [2] Kessler, D. J., Johnson, N. L., Liou, J. C., & Matney, M. (2010). The kessler syndrome: implications to future
488 space operations. *Advances in the Astronautical Sciences*, 137(8), 2010.
- 489 [3] Alvarez, J., & Walls, B. (2016). Constellations, clusters, and communication technology: Expanding small
490 satellite access to space. In *Aerospace Conference*, 2016 IEEE (pp. 1-11). IEEE.
- 491 [4] Karacalioglu, A. G., & Stupl, J. (2016). The Impact of New Trends in Satellite Launches on the Orbital Debris
492 Environment. *NASA Technical Report. Houston, TX, United States* (2016)
- 493 [5] Klinkrad, H. (2017). Large satellite constellations and related challenges for space debris mitigation. *J. Space*
494 *Saf. Eng.* 4, 59–60.
- 495 [6] Lewis, H.G., Radtke, J., Rossi, A., Beck, J., Oswald, M., Anderson, P., Bastida Virgili, B., Krag, H. (2017).
496 Sensitivity of the space debris environment to large constellations and small satellites. In: *Proc. 7th European*
497 *Conference on Space Debris*, Darmstadt, Germany.
- 498 [7] Foreman, V. L., Siddiqi, A., & De Weck, O. (2017). "Large satellite constellation orbital debris impacts: Case
499 studies of oneweb and spacex proposals." *AIAA SPACE and Astronautics Forum and Exposition*. (p. 5200).
- 500 [8] Olivieri, L., & Francesconi, A. (2020). Large constellations assessment and optimization in LEO space debris
501 environment. *Advances in Space Research*, 65(1), 351-363.
- 502 [9] Radtke, J., Kebschull, C., Stoll, E. (2017). Interactions of the space debris environment with mega
503 constellations—using the example of the oneweb constellation. *Acta Astronaut.* 131, 55–68.
- 504 [10] Rossi, A., Alessi, E.M., Valsecchi, G.B., Lewis, H., Radtke, J., Bombardelli, C., Virgili, B.B. (2017). A
505 quantitative evaluation of the environmental impact of the mega constellations. In: *Proc. 7th European*
506 *Conference on Space Debris*, Darmstadt, Germany.
- 507 [11] Virgili, B., Dolado, J., Lewis, H., Radtke, J., Krag, H., Revelin, B., Cazaux, C., Colombo, C., Crowther, R., Metz,
508 M. (2016). Risk to space sustainability from large constellations of satellites. *Acta Astronaut.* 126, 154–162.
- 509 [12] McKnight, D., Di Pentino, F., & Knowles, S. (2014). Massive Collisions In LEO - A Catalyst To Initiate ADR.
510 In: *Proc. 65th International Astronautical Congress*, Toronto, CA.
- 511 [13] Secure World Foundation, 2009 Iridium-Cosmos Collision Fact Sheet, last updated Nov. 10, 2010.
512 https://swfound.org/media/6575/swf_iridium_cosmos_collision_fact_sheet_updated_2012.pdf
- 513 [14] Letizia, F., Colombo, C., Lewis, H. G., & Krag, H. (2018). Development of a debris index. In *Stardust Final*
514 *Conference* (pp. 191-206). Springer, Cham.
- 515 [15] Letizia, F., Colombo, C., Lewis, H., & Krag, H. (2017). Extending the ECOB space debris index with
516 fragmentation risk estimation. In: *Proc. 7th European Conference on Space Debris*, Darmstadt, Germany.
- 517 [16] McKnight D., Speaks S., Macdonald J., Ebright K. (2018). Assessing Potential for Cross-Contaminating Breakup
518 Events from LEO to MEO/GEO. In: *Proc. 69th International Astronautical Congress*, Bremen, Germany.
- 519 [17] Olivieri L., Giacomuzzo C., Duran C., Giudici L., Colombo C. and Francesconi A. Investigation of ENVISAT
520 catastrophic fragmentation scenarios. *IAC 2021*, Dubai, 2021
- 521 [18] Ravi, P., Frueh, C., & Schildknecht, T. (2021). Investigation of three recent Atlas V Centaur upper stage
522 fragmentation events. In *8th European Conference on Space Debris* (Vol. 8).
- 523 [19] Frey, S., & Colombo, C. (2021). Transformation of satellite breakup distribution for probabilistic orbital collision
524 hazard analysis. *Journal of Guidance, Control, and Dynamics*, 44(1), 88-105.
- 525 [20] Pardini, Carmen, and Luciano Anselmo. "Evaluating the impact of space activities in low earth orbit." *Acta*
526 *Astronautica* 184 (2021): 11-22.
- 527 [21] Rossi, A., et al. "The H2020 ReDSHIFT project: a successful European effort towards space debris mitigation".
528 In *70th International Astronautical Congress (IAC 2019)*, Washington, D.C., USA.
- 529 [22] Henning, G. A., Sorge, M. E., Peterson, G. E., Jenkin, A. B., Mains, D., & McVey, J. P. (2019). "Parameterizing
530 Large Constellation Post-Mission Disposal Success to Predict the Impact to Future Space
531 Environment". *LPICo*, 2109, 6037.
- 532 [23] Liou, J. C. (2011). "An active debris removal parametric study for LEO environment remediation". *Advances in*
533 *Space Research*, 47(11), 1865-1876.
- 534 [24] Shan, M., Guo, J., & Gill, E. (2016). "Review and comparison of active space debris capturing and removal
535 methods". *Progress in Aerospace Sciences*, 80, 18-32.

- 536 [25] Brown, O., Niederstrasser, C., & Peterson, G. (2017) Space Traffic Safety: A New Self-Governance Approach
 537 for the Smallsat Community. In *31st Annual AIAA/USU Conference on Small Satellites*, Logan, UT, USA.
- 538 [26] Muelhaupt, T. J., Sorge, M. E., Morin J. & Wilson, R.S. (2019) Space traffic management in the new space era.
 539 *Journal of Space Safety Engineering*, 6(2), 80-87.
- 540 [27] Stokes, H., et al. (2019, December) Evolution of ISO's Space Debris Mitigation Standards. In 1st First
 541 International Orbital Debris Conference (IOC), Sugar Land, TX, USA.
- 542 [28] Wouters, J., De Man, P. & Hansen, R. (2016). Space debris remediation, its regulation and the role of Europe.
 543 *Eur. J.L Reform*, 18, 66.
- 544 [29] Lascombes, P. (2018). Electric propulsion for small satellites orbit control and deorbiting: The example of a Hall
 545 Effect thruster. In *2018 SpaceOps Conference* (p. 2729).
- 546 [30] OKNINSKI, A. (2021). Solid rocket propulsion technology for de-orbiting spacecraft. *Chinese Journal of*
 547 *Aeronautics*.
- 548 [31] Underwood, C., Viquerat, A., Schenk, M., Taylor, B., Massimiani, C., Duke, R., ... & Denis, A. (2019). InflateSail
 549 de-orbit flight demonstration results and follow-on drag-sail applications. *Acta Astronautica*, 162, 344-358.
- 550 [32] Rhatigan, J. L., Lan, W. D., Herrera, L., & Romano, M. (2019). Drag-Enhancing Deorbit Devices for Spacecraft
 551 Self-Disposal: A Review of Progress and Opportunities. *LPI Contributions*, 2109, 6124.
- 552 [33] Liu, J., Zhan, X., Li, G., Wang, Q., & Wang, S. (2020). Dynamics of orbital boost maneuver of low Earth orbit
 553 satellites by electrodynamic tethers. *Aerospace Systems*, 3, 189-196.
- 554 [34] Sato, T., Kawamoto, S., Watanabe, T., Kamachi, K., Ohkawa, Y., Oikawa, Y., ... & Okubo, H. (2021). A Study
 555 on PMD Device for Microsatellites Using Electrodynamic Tether. *TRANSACTIONS OF THE JAPAN SOCIETY*
 556 *FOR AERONAUTICAL AND SPACE SCIENCES, AEROSPACE TECHNOLOGY JAPAN*, 19(1), 61-67.
- 557 [35] Ahedo, E., & Sanmartin, J. R. (2002). Analysis of bare-tether systems for deorbiting low-earth-orbit
 558 satellites. *Journal of Spacecraft and Rockets*, 39(2), 198-205.
- 559 [36] Sanchez-Arriaga, J., Sanmartin, J.R. & Lorenzini, E.C. (2017) Comparison of technologies for deorbiting
 560 spacecraft from low-earth-orbit at end of mission, *Acta Astronautica*, 138, 536-542.
- 561 [37] G. Sarego, L. Olivieri, A. Valmorbida, A. Brunello, G. Colombatti, E. C. Lorenzini and G. Sanchez-Arriaga.
 562 "Impact risk assessment of deorbiting strategies in Low Earth Orbits," AIAA 2021-4243. ASCEND 2021.
 563 November 2021.
- 564 [38] Satomi Kawamoto, Nobuaki Nagaoka, Tsuyoshi Sato, Toshiya Hanada, Impact on collision probability by post
 565 mission disposal and active debris removal, *Journal of Space Safety Engineering*, Volume 7, Issue 3, 2020, Pages
 566 178-191, ISSN 2468-8967, <https://doi.org/10.1016/j.jsse.2020.07.012>.
- 567 [39] FET OPEN project, Electrodynamic Tether Technology for Passive Consumable-less Deorbit Kit (E.T.PACK),
 568 No. 828902, 1/3/2019-31/5/2022, <https://etpack.eu/>.
- 569 [40] L. Tarabini Castellani, S. Garcia González, A. Ortega, S. Madrid, E.C. Lorenzini, L. Olivieri, G. Sarego, A.
 570 Brunello, A. Valmorbida, M. Tajmar, C. Drobny, J-P. Wulfkuehler, R. Nerger, K. Wätzig, S. Shahsavani, G.
 571 Sánchez-Arriaga, Deorbit kit demonstration mission, *Journal of Space Safety Engineering*, 2022, ISSN 2468-
 572 8967, <https://doi.org/10.1016/j.jsse.2022.01.004>.
- 573 [41] J. D. Williams, J. R. Sanmartin and L. P. Rand, "Low Work-Function Coating for an Entirely Propellantless Bare
 574 Electrodynamic Tether," in *IEEE Transactions on Plasma Science*, vol. 40, no. 5, pp. 1441-1445, May 2012, doi:
 575 10.1109/TPS.2012.2189589.
- 576 [42] Sanchez-Arriaga, G. & Chen, X. (2018). Modeling and Performance of Electrodynamic Low-Work-Function
 577 Tethers with Photoemission Effects. *Journal of Propulsion and Power*, 34(1), pp. 213–220, January 2018. doi:
 578 10.2514/1.B36561.
- 579 [43] TEPCE 1,2 on Gunter's Space Page. https://space.skyrocket.de/doc_sdat/tepcce.htm (accessed 31.08.20).
- 580 [44] Khan, S. B., & Sanmartin, J. R. (2014). Analysis of tape tether survival in LEO against orbital debris. *Advances*
 581 *in space research*, 53(9), 1370-1376.
- 582 [45] Sanmartin, J. R., Sanchez-Torres, A., Khan, S. B., Sanchez-Arriaga, G., and Charro, M., "Optimum Sizing of
 583 Bare-Tape Tethers for De-Orbiting Satellites at End of Mission," *Advances in Space Research*, Vol. 56, No. 7,
 584 2015, pp. 1485–1492. doi:10.1016/j.asr.2015.06.030.
- 585 [46] Fujiwara, Michihiro, et al. Damage assessment for electrodynamic tape tether against space debris impact.
 586 *Transactions of the Japan society for aeronautical and space sciences, Aerospace Technology Japan* 19.1 (2021):
 587 34-41.
 588

- 589 [47] Sanmartin, Juan, Enrico Lorenzini, and Manuel Martinez-Sanchez. "A review of electrodynamic tethers for space
590 applications." 44th AIAA/ASME/SAE/ASEE Joint Propulsion Conference & Exhibit. 2008.
- 591 [48] Sanmartin, J. R., Lorenzini, E. C., & Martinez-Sanchez, M. (2010). Electrodynamic tether applications and
592 constraints. *Journal of Spacecraft and Rockets*, 47(3), 442-456.
- 593 [49] Siguier, J.M., Sarrailh, P., Roussel, J.F., Inguibert, V., Murat, G., Sanmartín, J., "Drifting Plasma Collection by
594 a Positive Biased Tether Wire in LEO-Like Plasma Conditions: Current Measurement and Plasma Diagnostic",
595 IEEE Transactions on Plasma Science 41, 3380-3386, 2013.
- 596 [50] Yao P, Sands T. Micro Satellite Orbital Boost by Electrodynamic Tethers. *Micromachines* (Basel). 2021 Jul
597 31;12(8):916. doi: 10.3390/mi12080916. PMID: 34442538; PMCID: PMC8400572.
- 598 [51] Bell I.C., Gilchrist B.E., McTernan J.K., Bilén S.G. Investigating miniaturized electrodynamic tethers for
599 picosatellites and femtosatellites, (2017) *Journal of Spacecraft and Rockets*, 54 (1), pp. 55 – 66, DOI:
600 10.2514/1.A33629.
- 601 [52] Shastri et. al., "Exploring Potential of Electrodynamic Tethers and Developments in the Miniature Tether
602 Electrodynamic Experiment", AIAA/USU Small Satellite Workshop, Logan, UT, Aug. 2014.
- 603 [53] Yasushi Ohkawa, Satomi Kawamoto, Tepei Okumura, Kentaro Iki, Hiroyuki Okamoto, Koichi Inoue, Takashi
604 Uchiyama, Daisuke Tsujita, Review of KITE – Electrodynamic tether experiment on the H-II Transfer Vehicle,
605 *Acta Astronautica*, Volume 177, 2020, Pages 750-758, ISSN 0094-5765,
606 <https://doi.org/10.1016/j.actaastro.2020.03.014>.
- 607 [54] Tsuyoshi Sato, Satomi Kawamoto, Yasushi Ohkawa, Takeo Watanabe, Koh Kamachi, Hiroshi Okubo,
608 Performance of EDT system for deorbit devices using new materials, *Acta Astronautica*, Volume 177, 2020,
609 Pages 813-820, ISSN 0094-5765, <https://doi.org/10.1016/j.actaastro.2020.01.029>.
- 610 [55] Kentaro Iki, Satomi Kawamoto, Yoshiki Morino, Experiments and numerical simulations of an electrodynamic
611 tether deployment from a spool-type reel using thrusters, *Acta Astronautica*, Volume 94, Issue 1, 2014, Pages
612 318-327, ISSN 0094-5765, <https://doi.org/10.1016/j.actaastro.2013.03.024>.
- 613 [56] Sanmartin, J. R., Martinez-Sanchez, M., and Ahedo, E., "Bare Wire Anodes for Electrodynamic Tethers", *Journal*
614 *of Propulsion Power*, Vol. 9, No. 3, 1993, pp. 353–360. doi:10.2514/3.23629.
- 615 [57] G. Sarego, A. Valmorbida, L. Olivieri, A. Brunello, G. Colombatti, M. Salmaso and E. C. Lorenzini,
616 "COLLISION AVOIDANCE MANEUVERS FOR SPACE TETHER SYSTEMS", Proceedings of the 3rd IAA
617 Conference on Space Situational Awareness (ICSSA), Madrid, Spain, April 2022.
- 618 [58] Francesconi A, Giacomuzzo C, Branz F, and Lorenzini E.C. (2013) *Survivability to hypervelocity impacts of*
619 *electrodynamic tape tethers for deorbiting spacecraft in LEO*. In 6th European Conference on Space Debris,
620 April 22-25, Darmstadt, Germany.
- 621 [59] G. Sánchez-Arriaga, L. Tarabini Castellani, E. C. Lorenzini, M. Tajmar, K. Wätzig, and A. Post, "Status of
622 development of a deorbit device based on electrodynamic tether technology in the E.T.PACK project", 8th
623 European Conference on Space Debris, ESA/ESOC, Virtual Conference, 20 – 23 April 2021, Darmstadt,
624 Germany.
- 625 [60] Jung, W., Mazzoleni, A.P. and Chung, J. "Nonlinear dynamic analysis of a three-body tethered satellite system
626 with deployment/retrieval". *Nonlinear Dynamics*, Vol. 82, pages 1127–1144 (2015).
627 <https://doi.org/10.1007/s11071-015-2221-z>.
- 628 [61] Christopher Murray and Matthew P. Cartmell, "Orbital-attitude coupling effects on the motion of a dumbbell
629 space tether", *Int. J. Space Science and Engineering*, Vol. 3, No. 2, pages 93-112, 2015.
- 630 [62] Ralph Caldecott, Dayangku NS Kamarulzaman, James P Kirrane, Matthew P Cartmell, Olga A Ganilova, "The
631 mechanics of motorised momentum exchange tethers when applied to active debris removal from LEO", *AIP*
632 *Conference Proceedings*, Volume 1637, Issue 1, pages 150-164, 2014. doi: 10.1063/1.4904574.
- 633 [63] Bettanini, C., Lorenzini, E. C., Colombatti, G., Aboudan, A., & Massironi, M. (2018). CUTIE: A cubesats tether-
634 inserted mission for moon exploration. *Acta Astronautica*, 152, 580-587.
- 635 [64] Inria Saclay Team Commands. Bocop: an open source toolbox for optimal control, 2017. URL <http://bocop.org>.
- 636 [65] Sarego, Giulia, et al. "Deployment requirements for deorbiting electrodynamic tether technology." *CEAS Space*
637 *Journal*, Vol. 13, Issue 4, 567 – 581 (2021).
- 638 [66] The Bare Electrodynamic Tethers Project (BETs), 01 Nov 2010, <https://www.thebetsproject.com> (accessed
639 28.09.21).
- 640 [67] Olivieri, L., Brunello, A., Sarego, G., Valmorbida, A., & Lorenzini, E. C. (2021). An in-line damper for tethers-
641 in-space oscillations dissipation. *Acta Astronautica*, Vol. 189, 559–566 (2021).

- 642 [68] Mantellato, R., Pertile, M., Colombatti, G., Valmorbida, A., Lorenzini, E.C. “Two-bar model for free vibrations
643 damping of space tethers by means of spring-dashpot devices”, (2014) CEAS Space Journal, 6 (3-4), pp. 133-
644 143.
- 645 [69] N.A. Ismail, M.P. Cartmell, “Three dimensional dynamics of a flexible Motorised Momentum Exchange Tether”,
646 Acta Astronautica, Volume 120, 2016, Pages 87-102, ISSN 0094-5765,
647 <https://doi.org/10.1016/j.actaastro.2015.12.001>.
- 648 [70] Zanuto Denis, “Analysis of Propellantless Tethered System for the De-Orbiting of Satellites at End of Life”, PhD
649 Thesis, University of Padova, 2013. <http://hdl.handle.net/11577/3422590>.
- 650 [71] The International Reference Ionosphere (IRI), <http://irimodel.org/> (accessed 28.09.21).
- 651 [72] International Geomagnetic Reference Field : 11th Generation,
652 <https://www.ncei.noaa.gov/access/metadata/landing->
653 [page/bin/iso?id=gov.noaa.ngdc.mgg.geophysical_models:IGRF-11](https://www.ncei.noaa.gov/access/metadata/landing-page/bin/iso?id=gov.noaa.ngdc.mgg.geophysical_models:IGRF-11) (accessed 28.09.21).
- 654 [73] J.M. Picone, A.E. Hedin, D.P. Drob, A.C. Aikin, NRLMSISE-00 empirical model of the atmosphere: Statistical
655 comparisons and scientific issues, Journal of Geophysical Research: Space Physics, 107 (A12), (2002) 1468.
- 656 [74] E. Hairer, RADAU code at Genève University, <http://www.unige.ch/~hairer/prog/stiff/radau5.f> (accessed
657 28.09.21).
- 658 [75] E. Hairer, DOPRI code at Genève University, <http://www.unige.ch/~hairer/prog/nonstiff/dopri5.f> (accessed
659 28.09.21).
- 660 [76] A. Valmorbida, M. Mazzucato, S. Tronco, S. Debei, E.C. Lorenzini, “SPARTANS — a cooperating spacecraft
661 testbed for autonomous proximity operations experiments”, IEEE instrumentation and measurement technology
662 conference, vol 2015–July 2015
- 663 [77] Valmorbida, A., Scarpa, F., Mazzucato, M., Tronco, S., Debei, S., Lorenzini, E.C., “Attitude Module
664 characterization of the Satellite Formation Flight testbed”, in *Proceedings of 2014 IEEE International Workshop*
665 *on Metrology for Aerospace*, (MetroAeroSpace), art. no. 6865897, pp. 73-78, 2014.
- 666 [78] A. Brunello, L. Olivieri, G. Sarego, A. Valmorbida, E. Lungavia, E.C. Lorenzini, “*Space Tethers: parameters*
667 *reconstruction and Tests*”, “IEEE International Workshop on Metrology for Aerospace”, Proceedings of the
668 virtual conference.
- 669 [79] Petrillo, Davide, et al. Flexible Electromagnetic Leash Docking system (FELDs) experiment from design to
670 microgravity testing. *66Th International Astronautical Congress*, IAC-15 E. Vol. 2. 2015.
- 671 [80] G. Grassi, A. Gloder, L. Pellegrina, et al., “An innovative space tether deployer with retrieval capability: Design
672 and test of STAR experiment,” *Proceedings of the 68th IAC, Adelaide, Australia*, pp. 25–29, 2017.
- 673 [81] L. Olivieri, A. Valmorbida, G. Sarego, et al. Test of tethered deorbiting of space debris. *Advances in Astronautics*
674 *Science and Technology*, vol. 3, no. 2, pp. 115–124, 2020.
- 675 [82] Valmorbida, Andrea, et al. Experimental Validation of a Deployment Mechanism for Tape-tethered
676 Satellites. *2021 IEEE 8th International Workshop on Metrology for AeroSpace (MetroAeroSpace)*. IEEE, 2021.
- 677 [83] J. Peláez, M. Ruiz Delgado, E.C. Lorenzini, Strategies for maximizing a satellite lifetime by tether-mediated
678 orbital injection, *J. Astronaut. Sci.* 45(2), 205–231, 1997.
- 679 [84] Zhong, R., and Z. H. Zhu. "Long-term libration dynamics and stability analysis of electrodynamic tethers in
680 spacecraft deorbit." *Journal of Aerospace Engineering* 27.5 (2014): 04014020.
- 681 [85] R. Zhong, Z.H. Zhu, “Long term dynamics and optimal control of nano-satellite deorbit using a short
682 electrodynamic tether”, *Advances in Space Research*, Volume 52, Issue 8, 2013, Pages 1530-1544, ISSN 0273-
683 1177, <https://doi.org/10.1016/j.asr.2013.07.031>.
- 684 [86] Pelaez J., Lorenzini E.C., Lopez-Rebollal O., Ruiz M. “A New Kind of Dynamic Instability in Electrodynamic
685 Tethers.” *The Journal of the Astronautical Sciences* Vol. 48, No. 4, 449-476, 2000.
- 686